

Relationship between microstructure of plasma-sprayed 8YZ coatings and thermal fatigue life of thermal barrier coatings

K. YASUDA, S. SUENAGA, H. INAGAKI, Y. GOTO, H. TAKEDA
Power Supply Materials and Devices Laboratory, Corporate Research and Development Center, Toshiba Corporation, 1, Komukai, Toshiba-cho, Saiwai-ku, Kawasaki 210-8582, Japan
 E-mail: kazuhiko-yasuda@toshiba.co.jp

K. WADA
Power and Industrial Systems Research and Development Center, Toshiba Corporation, Yokohama 235-0045, Japan

Microstructure of plasma-sprayed yttria-stabilized zirconia coatings (8YZ) was characterized by the measurement of surface roughness, hardness, and pore size distribution and was correlated with thermal fatigue life. It was confirmed that the coatings which had greater roughness tended to show both lower hardness and higher porosity. Furthermore, such coatings were found to have a longer thermal fatigue life. We propose that measurement of the roughness of 8YZ coatings is useful as a non-destructive evaluation method for predicting thermal fatigue life. © 2000 Kluwer Academic Publishers

1. Introduction

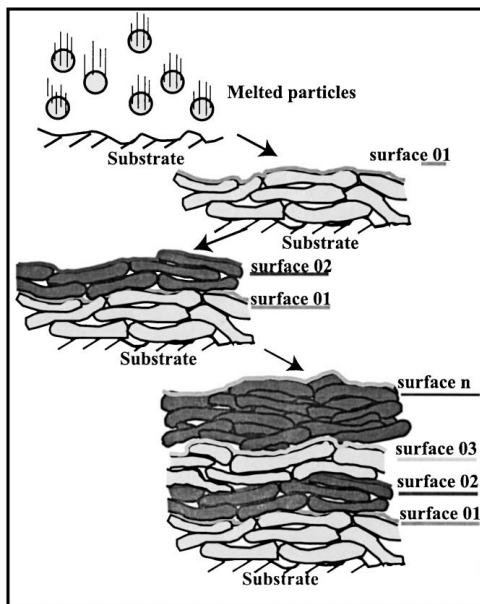
Plasma-sprayed ceramic coatings have been applied as thermal barrier coatings (TBCs) on gas turbine components [1]. TBCs are composed of a ceramic coating and a metal (MCrAlY, M = Ni, Co) coating on Ni or Co superalloy. In order to enhance the efficiency of power generation, gas turbine temperatures have tended to increase. For this reason, the importance of the ceramic coatings is becoming more important. Yttria-stabilized zirconia has been adopted as a ceramic coating because of its low thermal conductivity and high thermal expansion coefficient.

Failure of zirconia coatings has been a serious problem when TBCs are used for gas turbine components. Failure has occurred at the interface between the zirconia and metal layers, particularly on the inside of the zirconia layer [2, 3]. Failure of the plasma-sprayed coatings was reported to be related to the microstructure of the coatings [4–6]. To prevent such failure, characterization of zirconia coatings has been carried out. To determine the microstructure of plasma-sprayed zirconia coatings, porosity and elastic modulus were measured. Because TBCs component consists of a metal substrate, a metal coating, and a zirconia coating, it is difficult to measure the properties of the zirconia coating directly. Furthermore, non-destructive evaluation of the microstructure of the zirconia coatings is advantageous. However, no practical procedure has been established so far.

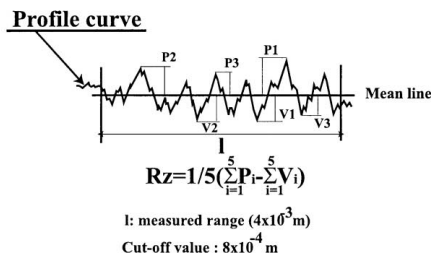
In this study, we introduce a new evaluation method for plasma-sprayed zirconia coatings in order to predict the thermal fatigue life of TBCs. Fig. 1 shows schemat-

ically the surface roughness of a typical coating after sprays. First, the melted particles collide the surface of substrate and surface 01 is formed. Next, surface 02 is formed on surface 01. In the same way, surface n is formed by n times of spraying passes of torch. Since, in our experiment, relatively the coarse powders were sprayed on a substrate having a rough surface, the surface of each sprayed coating layer, surface 01– n , was rough. As shown in Fig. 1, the plasma-sprayed coating is formed by accumulation due to the collision and solidification of melted powder particles. Furthermore, coatings with a thickness as large as 200–500 μm for TBCs were formed by several spraying passes of the torch. If it can be considered that the plasma-sprayed coating is composed of layers 01– n , it is speculated that characteristics, for example, roughness, of surface m ($m < n$) indicate the internal structure of the coating. Furthermore, if the characteristics of the surface m can be predicted by the observation of those of surface n , the characteristics of the surface n are expected to reflect the internal structure of the coatings. In this paper, the measurement of surface roughness was adopted as the characterization method of the surface of the sprayed layer. As shown in Fig. 1, the definition of typical roughness, R_z was also shown. Other roughness parameters, namely, R_a , R_{max} , R_t , R_{tm} are also generally used besides R_z . In this experiment, however, we adopted R_z because other parameters have the same behavior.

We surveyed the roughness, hardness, and pore size distribution of the zirconia coatings as a means of characterizing their microstructures. Furthermore,



a) Relationship between surface and internal structure



b) Definition of surface roughness (JIS B0601 1982)

Surface roughness of the coating after sprays

Figure 1 Surface roughness of plasma-sprayed coatings and definition of surface roughness (R_z).

we also investigated the relationship between the microstructure and thermal fatigue life in order to propose non-destructive evaluation procedures for plasma-sprayed coatings.

2. Experimental

Nickel base superalloy (IN738LC) specimens ($20 \times 20 \times 3$ mm) were prepared as substrates for TBCs. The TBCs were formed on the superalloy, after blasting with alumina grit, by the atmospheric plasma-spray (APS) method. The composition of the metal coating was NiCoCrAlY (Ni-23Co-16Cr-12Al-0.6Y; mass %). The composition of the ceramic coating was 8 mass % Y_2O_3 - ZrO_2 . The plasma-spray conditions are shown in Table I. Powder is injected into the inside of gun. Six kinds of powders with different particle size distributions and powder preparation methods were used for ceramic coatings (Table II). The thicknesses of metal and zirconia coatings were 150 and 250 μm , respectively.

To characterize the microstructure of the zirconia coatings, their surface roughnesses were measured. For three characteristic zirconia coatings (8YZA, 8YZE and 8YZF), in particular, the surface roughnesses which were formed after each of several spray passes were measured [7]. In order to investigate the influence of the

TABLE I Plasma-spray conditions

Parameter	Metal coating	Ceramic coating
Arc current	850 A	900 A
Arc voltage	37 V	37 V
Gas pressure		
Ar	0.34 MPa	0.34 MPa
He	0.34 MPa	0.34 MPa
Spray distance	12.5×10^{-2} m	12.5×10^{-2} m

Gun; SG-100(Plasmadyne), System; 3600-40, Powder injection point; inside of gun, Spray angle; normal to substrate.

TABLE II Zirconia spray powders

Powders	Preparation	Particle size (μm)
8YZA	AS	10–44
8YZB	AS	44–88
8YZC	A	44–88
8YZD	A Hollow powder	44–88
8YZE	FC	10–44
8YZF	FC	44–88

AS: agglomerated and sintered powder, A: agglomerated powder, FC: fused and crushed powder.

TABLE III Surface roughness of zirconia coatings all of 250 μm thickness, bond coating of 63.5 μm roughness, NiCoCrAlY

R_z (μm)	NiCoCrAlY	8YZA	8YZB	8YZC	8YZD	8YZE	8YZF
Average	63.54	64.86	57.52	57.98	52.03	38.63	51.29
Std. Dev.	4.60	4.98	3.30	4.04	8.87	3.56	8.16

surface roughness of the underlying NiCoCrAlY coating on the roughness of the zirconia coating, the 8YZA and 8YZE layers were formed on two NiCoCrAlY coatings with different surface roughnesses. The Vickers hardness (HV) of the zirconia coating was measured with a load of 200 g for 30 s. The measured layer was more than 50 μm above the interface between the metal and zirconia coatings. The pore size distribution of zirconia coatings was measured by mercury intrusion porosimetry (MIP). The coatings for MIP measurement were formed on SUS304 plates ($70 \times 50 \times 3$ mm, surface roughness; $R_z = 20.44 \mu\text{m}$ (Std. dev. = $1.67 \mu\text{m}$)) and thermal fatigue tests (TFTs) were carried out by holding the specimens for 30 min both at 150 and 1000 $^\circ\text{C}$ under atmospheric pressure. The thermal fatigue life was determined when the zirconia coating had separated from the metal coating.

3. Results and discussion

3.1. Roughness of zirconia coating

Table III shows the surface roughness of the NiCoCrAlY coating and zirconia coatings. Although zirconia coatings were sprayed on the NiCoCrAlY underlayer with the same surface roughness, the roughnesses obtained by the zirconia coatings from different powders were different. Comparing the coatings 8YZE and 8YZF, which were prepared by using fused and crushed powders, coating 8YZF formed from coarser powder had greater surface roughness. However, this tendency was not found in layers from agglomerated and sintered

powders; in these coatings, the surface roughness had no relation to the starting powder size distribution.

Fig. 2 shows the relationship between the surface roughness (R_z) and the layer thickness of coatings 8YZA, 8YZE and 8YZF. The surface roughness of 8YZE and 8YZF decreased with an increase in thickness, while that of 8YZA was constant. While R_z of the coatings from the fused and crushed powders initially decreased with additional spray passes, their roughness became constant value for more than 100 μm thickness. The results shown in Table III and Fig. 2 suggest that the surface roughness of the zirconia coating after multiple spray passes reflected the state of the piling up of the melted powder particles and was dependent on the characteristics of the plasma-spray powders.

Table IV shows the relationship between the surface roughnesses of the zirconia coatings and those of the NiCoCrAlY coatings. The surface roughnesses of zir-

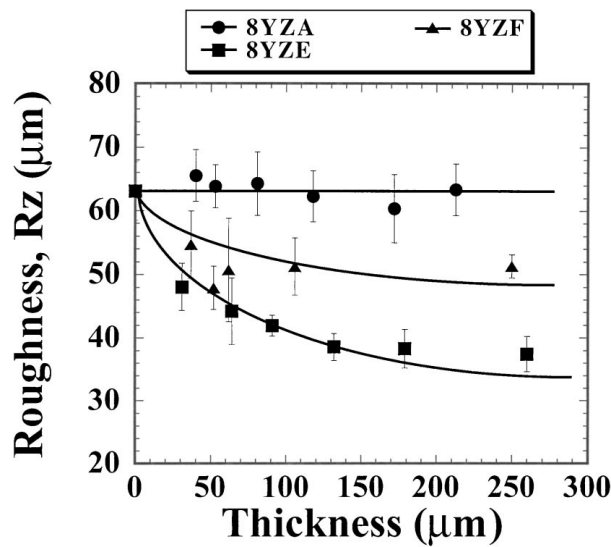


Figure 2 Relationship between surface roughness and thickness of plasma-sprayed zirconia coatings deposited on a NiCoCrAlY bond coating of 63.5 μm roughness.

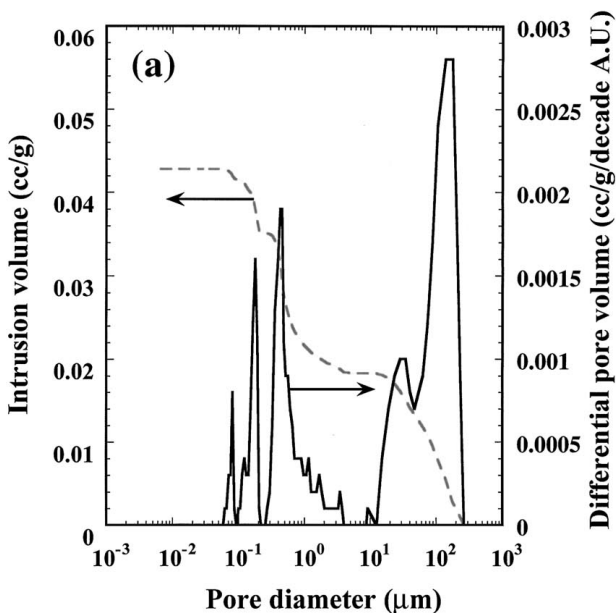


TABLE IV Relationship between surface roughnesses of zirconia coatings of 250 μm thickness and those of the NiCoCrAlY bond coatings

NiCoCrAlY	R_z (μm)	Std. Dev.	R_z (μm)	Std. Dev.
	63.54	4.60	29.57	3.51
8YZA	64.86	4.98	62.48	6.93
8YZE	38.63	3.56	36.26	3.03

conia coatings were independent of the roughness of the metal coating. These results suggest that, regardless of the surface roughness of the NiCoCrAlY coating, the surface roughness of zirconia coatings thicker than 100 μm indicated how the melted powder particles were piled up during the spraying procedure.

3.2. Pore size distribution

Fig. 3 shows the pore size distributions of both 8YZA and 8YZE with thicknesses of 260 and 270 μm , respectively, as determined by MIP measurements. The total porosities of 8YZA and 8YZE were 19.8 and 12.8%, respectively. The plasma-sprayed ceramic coatings usually have two major peaks in the pore size distribution, i.e., in the region lower than 1 μm and in the region above 10 μm . Senda *et al.* reported that the former originated from the small pores and microcracks within the flattened particles and the latter from the large pores between the flattened particles [8]. The results shown in Figs 2 and 3 suggest that the zirconia coatings which had been sprayed to form a high roughness tended to have higher porosity due to interparticle pores and that the coatings which were sprayed to form a low roughness tended to have lower porosity due to reduced interparticle pores.

3.3. Vickers hardness

Fig. 4 shows the relationship between the Vickers hardness and roughness of the zirconia coatings. The Vickers hardness ranged from 364.1 HV (3.57 GPa) to 826.8 HV (8.10 GPa) and decreased with an increase

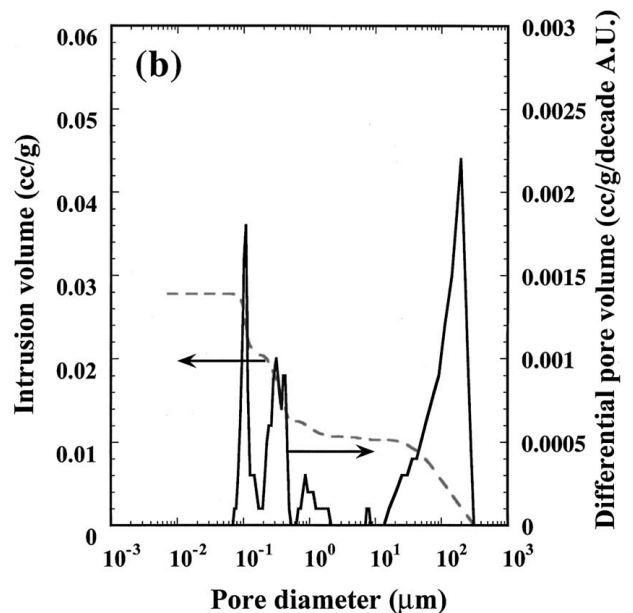


Figure 3 Pore distribution of plasma-sprayed zirconia coatings (a) 8YZA, (b) 8YZE.

in roughness. It has been reported that hardness is proportional to the elastic modulus [9]. The relationship shown in Fig. 4 thus means that the greater the surface roughness of the zirconia coatings, the lower the elastic modulus.

Fig. 5 shows the indentation of a Vickers indenter in plasma-sprayed coatings (8YZA and 8YZE) under 500 gf for 30 s. In 8YZA, several cracks were seen around the indentation and they ran through the intergranular pores between flattened particles. While, there were no cracks around indentation in 8YZE. These photos suggest that the stress required to generate cracks in 8YZE is greater than that in 8YZA.

3.4. Relationship between thermal fatigue life and microstructure of the zirconia coatings

Fig. 6 shows the relationship between the surface roughness and thermal fatigue life of the 8YZ coatings. It was

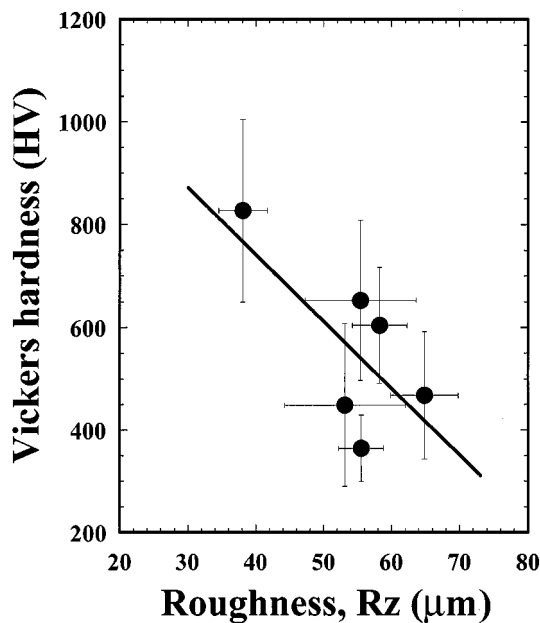
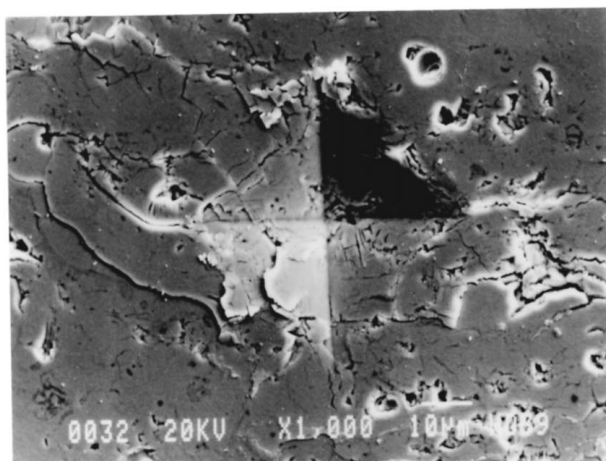
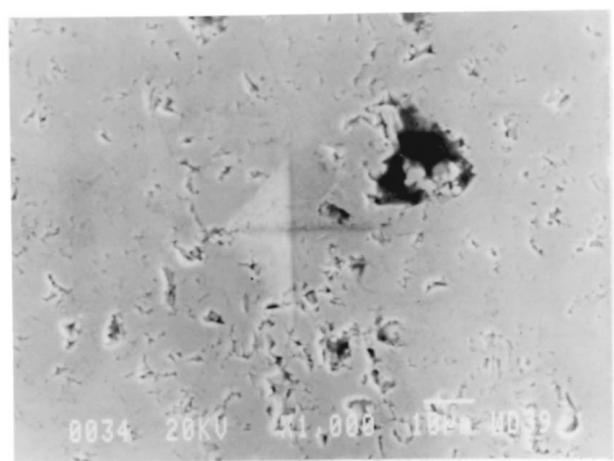


Figure 4 Relationship between Vickers hardness (HV_{0.2 kgf}) and roughness (R_z).



(a)



(b)

Figure 5 Indentation of Vickers indenter in the cross section of plasma-sprayed coatings. (a) 8YZA, (b) 8YZE.

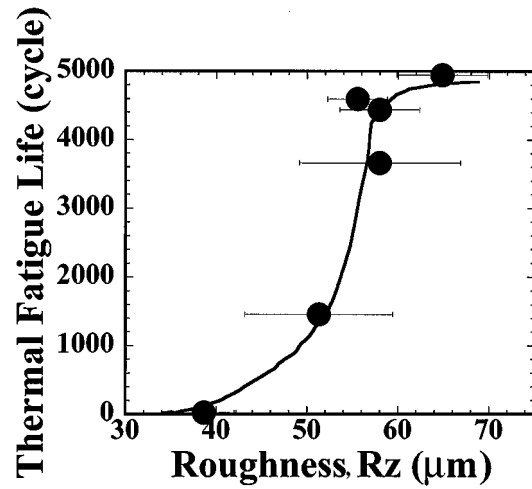


Figure 6 Relationship between thermal fatigue life and roughness of plasma-sprayed coatings.

seen that the thermal fatigue life was roughly proportional to the surface roughness of the coatings. The coatings with high thermal fatigue life had surface roughness (R_z) greater than 55 μm.

The thermal fatigue life of the TBCs was mainly determined by the failure in the ceramic coating near the metal coating. This failure resulted from thermal stress due to the difference in the coefficients of thermal expansion (CTE) between the coating and substrate during cooling. When the film is thin, this stress (σ) can be approximated by

$$\sigma_r = \frac{E \Delta\alpha \Delta T}{1 - \nu^2} \quad (1)$$

where Δα is the difference between the CTEs of the coating and substrate, E and ν are the elastic modulus and Poisson's ratio of the coating, and ΔT is the temperature difference between the soak temperature and ambient. From Equation 1, it is obvious that a decrease in E makes σ lower. As shown in Figs 3 and 4, the coatings which had formed with high roughness had lower Vickers hardness and sufficient interparticle pores. Furthermore, from the relationship between Vickers hardness and the elastic modulus, plasma-sprayed coatings formed with greater roughness have a lower elastic

modulus. These results suggest that the long fatigue lives of zirconia coatings with great roughness could be explained by decrease of the stress that associated with failure of the coating from a lower elastic modulus of coatings. On the other hand, as shown in Fig. 5, cracks around the indentation suggested that plasma-sprayed coatings which had a lower Vickers hardness would also have a lower fracture strength. While, the results of Figs 5 and 6 indicated that these TFT lives were long in spite of lower fracture strength. For these reasons, we suggest that the decrease in stress originating from the difference in CTEs is due to the decrease in the elastic modulus of the zirconia coating, which contributes to its longer TFT life under this TFT condition.

According to the results of this investigation, the measurement of the surface roughness of the zirconia coating is a useful non-destructive evaluation method for predicting thermal fatigue life.

4. Conclusion

The roughness, hardness and pore size distribution of plasma-sprayed yttria-stabilized zirconia coatings were measured in order to characterize the microstructure and to investigate their relationship to the thermal fatigue life of TBCs. The following findings were obtained.

1. The surface roughness of the plasma-sprayed zirconia coating reflected the state of the piling up of the melted powder particles, and its roughness was not

dependent on the surface roughness of the underlying metal bond coating.

2. Plasma-sprayed zirconia coatings with greater surface roughness tended to have a lower Vickers hardness and higher porosity.

3. In samples of 8YZ which had a roughness R_z greater than $55 \mu\text{m}$, a longer thermal fatigue life was observed.

Based on these results, it is concluded that the surface roughness of as-sprayed plasma-sprayed coatings reflects the internal microstructure of the coatings and that measurement of the roughness is a useful non-destructive evaluation method for predicting the thermal fatigue life.

References

1. S. STECURA, *Ceram. Bull.* **56** (1977) 1082.
2. B. CHEN and E. CHANG, *J. Amer. Ceram. Soc.* **72** (1989) 212.
3. A. H. BARLETT and R. D. MASCHIO, *ibid.* **78** (1995) 1018.
4. R. TAYLOR, J. R. BRANDON and P. MORRELL, *Surf. Eng.* **43/44** (1990) 470.
5. *Idem.*, *Surf. Coat. Tech.* **50** (1992) 141.
6. S. V. JOSHI and M. P. SRIVASTAVA, *Surf. Eng.* **11** (1995) 233.
7. JIS B0601.
8. T. SENDA, S. AMADA, S. UEMATSU and S. SATO, *J. Plasma-spray Soc. of JPN* **24** (1988) 8.
9. D. B. MARSHALL, T. NOMA and A. G. EVANS, *J. Amer. Ceram. Soc.* **65** (1982) C-175.

Received 18 January
and accepted 12 July 1999